Isotope effect on electron-phonon interaction in the multiband superconductor MgB_2

Daixiang Mou, Soham Manni, Valentin Taufour, Yun Wu, Lunan Huang, S. L. Bud'ko, P. C. Canfield, and Adam Kaminski
Division of Materials Science and Engineering, Ames Laboratory, Ames, Iowa 50011, USA
and Department of Physics and Astronomy, Iowa State University, Ames, Iowa 50011, USA
(Received 9 February 2016; published 7 April 2016)

We investigate the effect of isotope substitution on the electron-phonon interaction in the multiband superconductor MgB_2 using tunable laser-based angle-resolved photoemission spectroscopy. The kink structure around 70 meV in the σ band, which is caused by electron coupling to the E_{2g} phonon mode, is shifted to higher binding energy by ~3.5 meV in $Mg^{10}B_2$ and the shift is not affected by superconducting transition. These results serve as the benchmark for investigations of isotope effects in known, unconventional superconductors and newly discovered superconductors where the origin of pairing is unknown.

DOI: 10.1103/PhysRevB.93.144504

I. INTRODUCTION

The discovery of the isotope effect in conventional superconductor played a key role in establishing Bardeen-Cooper-Schrieffer (BCS) theory [1–4], in which electrons form Cooper pairs by coupling via lattice vibrations (phonons). The isotope effect is regarded as a decisive method to determine whether or not the pairing in newly discovered superconductors is phonon mediated or of unconventional (e.g., electron-electron) origin. This approach worked beautifully in the case of the MgB_2 superconductor [5,6] and immediately established electron-phonon coupling as the origin of pairing and superconductivity in this material [6]. The phonon-mediated superconductivity in this material was explained by multiband BCS/Eliashberg theory shortly after its discovery [6–9]. Similar measurements have been made on cuprate high-temperature superconductors, but no unambiguous conclusion has been reached because of the complexity of isotope response and inconsistent results [10–13]. Thus, MgB_2 is unique in its combination of very high T_c values and unambiguous electron-phonon coupling.

The electron-boson interaction renormalizes the binding energy of the electrons near chemical potential, causing a "kink" structure in the band dispersion, which is a signature of a sudden change of self-energy due to coupling to the bosonic mode. Angle-resolved photoemission spectroscopy (ARPES), a powerful tool that can measure the band dispersion and self-energy with momentum resolution, provides a direct way to study the electron-boson interaction. The kink structure in cuprate high-temperature superconductor has been intensively investigated by ARPES for years because it might contain essential information to establish the high-temperature superconducting mechanism [14]. But whether the observed kink is related to phonon or spin fluctuation is still an open question. There were several ARPES-based studies of the isotope effect in cuprates superconductors carried out in the past [15–18]. The results included observation of a very large change in band dispersion at high binding energies, interpreted as a signature of polaronic effects [15] and observation of very small effect at low energies along the nodal direction [18]. Due to difference in conclusions, the significance and relation to high-temperature superconductivity remains unclear. Surprisingly, to the best of our knowledge, no direct experimental study of the isotope effect on the kink structure in a classical BCS superconductor has been reported. MgB_2 offers a unique opportunity due to its relatively high T_c and its quasi-two-dimensional character of the σ bands.

MgB_2 is a layered multiband superconductor with a transition temperature as high as 40 K [5,6]. The strong electron-phonon interaction and discovery of the large isotope effect on T_c [6,7] make this material an ideal system for the investigation of this important topic and to establish benchmarks for gaining insights into novel superconductors. Early ARPES studies of MgB_2 did not reveal the kink structure because of experiment resolution and sample quality and size limitations [19–21]. Recently, the kink structure was identified using our tunable laser ARPES system with much-improved instrumental resolution [22,23]. This provides us with the opportunity to study the isotope effect on the kink structure in a prototypical conventional superconductor. In this paper, we report an ARPES study of the electron-phonon interaction in $Mg^{10}B_2$ and $Mg^{11}B_2$ samples. We will show the clear isotope shift of the kink structure on the σ band and that this isotope shift is not significantly affected by the superconducting transition.

II. EXPERIMENTAL DETAILS

MgB_2 single crystals are usually grown from a solution with excess Mg under high pressure and high temperature in boron nitride (BN) crucibles [24]. Unfortunately, for isotopic substitution, there are clear indications that BN is partly reacting with Mg during the high-pressure/high-temperature growth process. The incorporation of BN into the high-temperature melt is suggested by the growth of BN single crystals together with MgB_2 and is clearly implicated by the fact that MgB_2 crystals grown with nominally, isotopically pure ^{11}B contain detectable and enhanced levels of ^{10}B that appears to be coming from the BN crucibles made from natural abundance B [25]. To avoid any contamination from natural B contained in the BN crucible, we performed the MgB_2 growths using MgO crucibles. Under these conditions, only single crystals of MgB_2 form and the isotopic purity of B can be preserved. The success of these growths also demonstrates that MgB_2 single crystals can be grown from a binary melt when adequate pressure is used to both control vapor pressure and shift the phase lines in the binary phase diagram. Single crystals of both $Mg^{11}B_2$ and $Mg^{10}B_2$ were grown in the following manner using high-purity Mg as well as 99.5% isotopically pure ^{11}B and ^{10}B from Eagle

Pitcher. Elemental Mg and B were placed in a thin-walled MgO crucible in the ratio of Mg:B 1:0.7. Using a cubic anvil furnace, we apply around 3.5 GPa of pressure on the sample at room temperature, and then the temperature is increased to 1450 °C over approximately 2 h, after dwelling at 1450 °C for 2 h, the temperature is decreased to 650 °C over 6 h. At this point, the heater is turned off, quenching the growth to room temperature, and the pressure is decreased back to ambient. The MgO crucible is then removed from the pressure media and the excess Mg is distilled off of the MgB_2 crystals.

The typical size of the samples used in ARPES measurements was $\sim 0.3 \times 0.3 \times 0.2$ mm^3. Samples were cleaved *in situ* at a base pressure of lower than 8×10^{-11} Torr. ARPES measurements were carried out using a laboratory-based system consisting of a Scienta R8000 electron analyzer and tunable Vacuum Ultraviolet (VUV) laser light source [26]. The energy resolution of the analyzer was set at 1 meV and angular resolution was 0.13° and ∼0.5° along and perpendicular to the direction of the analyzer slits, respectively. All data were acquired using a photon energy of 6.7 eV; only the electronic structure of the two σ bands around the Brillouin zone center can be measured with this photon energy. Fortunately, it is the σ band that couples strongly with the phonons. The laser beam was focused to a spot with a diameter of ∼30 μm. Samples were cooled using a closed-cycle He refrigerator and the sample temperature was measured using a silicon-diode sensor mounted on the sample holder. The energy corresponding to the chemical potential was determined from the Fermi edge of a polycrystalline Au reference in electrical contact with the sample. In every temperature-dependent measurement, aging effects were checked by thermal cycling. The consistency of the data was confirmed by measuring several samples.

III. RESULTS AND DISCUSSION

Figure 1(a) shows the low-field temperature dependence of the magnetization for representative crystals of $Mg^{10}B_2$ and $Mg^{11}B_2$. A clear, approximately 1.0 K isotope shift is seen in these data. It should be noted that each transition is lower by approximately 1.0 K ($T_c(^{11}B) = 37.5$ K, $T_c(^{10}B) = 38.5$ K) from what was previously reported in Ref. [6]. This is due to the fact that the high-pressure growth requires the use of a graphite heater in close proximity to the Mg-B melt. This leads to a small carbon substitution (∼1%) that mildly suppresses T_c. The measured ARPES data in the superconducting state ($T = 15$ K) of ^{11}B and ^{10}B samples are shown in Figs. 1(b) and 1(c). We chose a particular cut position in the momentum space [see the measured Fermi surface in Fig. 2(a)] where the matrix element totally suppresses the intensity of the inner σ band to simplify the data analysis. The anomaly in the band dispersion

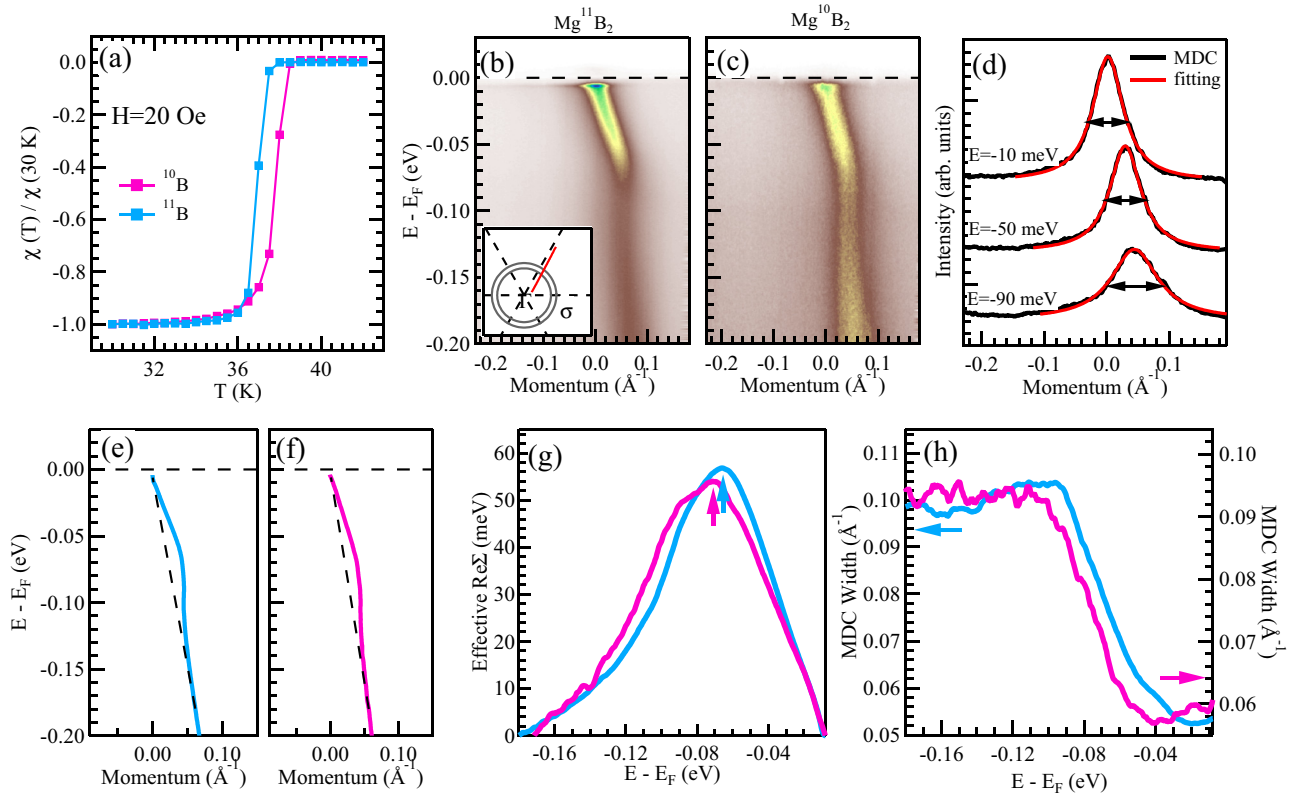

FIG. 1. Isotope effect on kink structure in MgB_2. (a) Temperature dependence of magnetic susceptibility of $Mg^{11}B_2$ and $Mg^{10}B_2$ single crystals used in ARPES measurements. [(b) and (c)] ARPES intensity plots for $Mg^{11}B_2$ and $Mg^{10}B_2$ samples along a cut that crosses the σ band measured at 15 K. (d) Momentum distribution curves (MDC) and Lorentzian fits at three sample binding energies. Horizontal arrows mark the MDC width that is proportional to ImΣ. (e) Band dispersion extracted by fitting the MDC data with Lorentzian function for $Mg^{11}B_2$ sample, as shown in panel (d). Dashed lines are corresponding bare bands used to extract the ReΣ. (f) Same as in (e) but for a $Mg^{10}B_2$ sample. (g) Effective ReΣ obtained by subtracting the "bare" band dispersion [dashed lines in (e) and (f)] from extracted dispersion. Kink positions are marked with arrows. (h) Energy dependence of the MDC width.

(kink) can be clearly seen directly in the the ARPES intensity plots around a binding energy of 70 meV and is caused by the coupling of the electrons to the E_{2g} phonon mode as discussed in our previous report [22].

In order to quantitatively analyze the details of this kink structure, we extracted the band dispersion by fitting the momentum distribution curves (MDC) with Lorentzian line shape as shown in Fig. 1(d). The resulting band dispersion is shown in Figs. 1(e) and 1(f) for samples containing each of the boron isotopes. The effective real part of self-energy (ReΣ) is then obtained by subtracting a linear "bare" band dispersion [plotted as a dashed lines in Figs. 1(e) and 1(f)] from the measured dispersion and shown in Fig. 1(g). The clearly visible peak is due to interaction of the electrons with the phonon mode. The shape of this peak is slightly asymmetric, which is due to fact that ReΣ is an antisymmetric function about E_F. The slight shoulder on the high-binding-energy side is most likely a reflection of complexity of electron-phonon interaction rather than a separate mode. The width of the MDC is a measure of the imaginary part of the self-energy (ImΣ) and is enhanced for the binding energies higher than the energy of the boson mode plus superconducting gap as plotted in Fig. 1(h). Both the shape of ReΣ [Fig. 1(g)] and the MDC width [Fig. 1(h)] show a shift toward higher binding energy in the ^{10}B sample, providing clear evidence of the strong isotope effect in this material. Theoretically, either the peak position in ReΣ or the midpoint of the dropping edge in ImΣ can be used to extract coupling boson mode energy, but the ReΣ is more accurately extracted from data fits (it is easier to extract peak position than its width) and is more commonly used in the literature [14]. The energy value of the ReΣ peak is 66.5 meV for the ^{11}B sample and 70 meV for the ^{10}B sample, respectively. Therefore the effects of different isotope mass on the energy of the phonon mode amounts to shift of ~3.5 meV

In order to confirm that the observed isotope energy shift does not arise due to some small angular misalignment associated with two measurement of two separate crystals, we measured the momentum dependence of the kink structure in both samples over a wide angular range. Following the same procedure as described above, we extracted the effective ReΣ along different cuts in momentum space in Fig. 2(b) (^{10}B sample) and Fig. 2(c) (^{11}B sample) and the momentum dependent kink energy in Fig. 2(d). The energy position of the kink structure is nearly momentum independent in both samples, demonstrating that the shift reported here of the kink energy attributed to the isotope effect is not due to an artificial caused by slight misalignment during measurement, which was a likely culprit in early isotope experiments in cuprates [15].

Finally, we turn to the temperature dependence of the isotope effect. We compare the extracted ReΣ of the outer σ band at different temperatures in Fig. 3(a). The shift of the peak structure is obvious for all measured temperatures up to 60 K. In Fig. 3(b), we extracted a temperature-dependent peak position of ReΣ in both samples. The temperature dependence of the kink position in ^{11}B samples was already discussed in our previous report [22]. The kink energy remains constant in the normal state and starts to shift to high binding energy gradually below T_c with a total shift of ~3 meV at the lowest measured temperature. The kink position in the ^{10}B sample has a similar temperature dependence as that in the ^{11}B sample and also

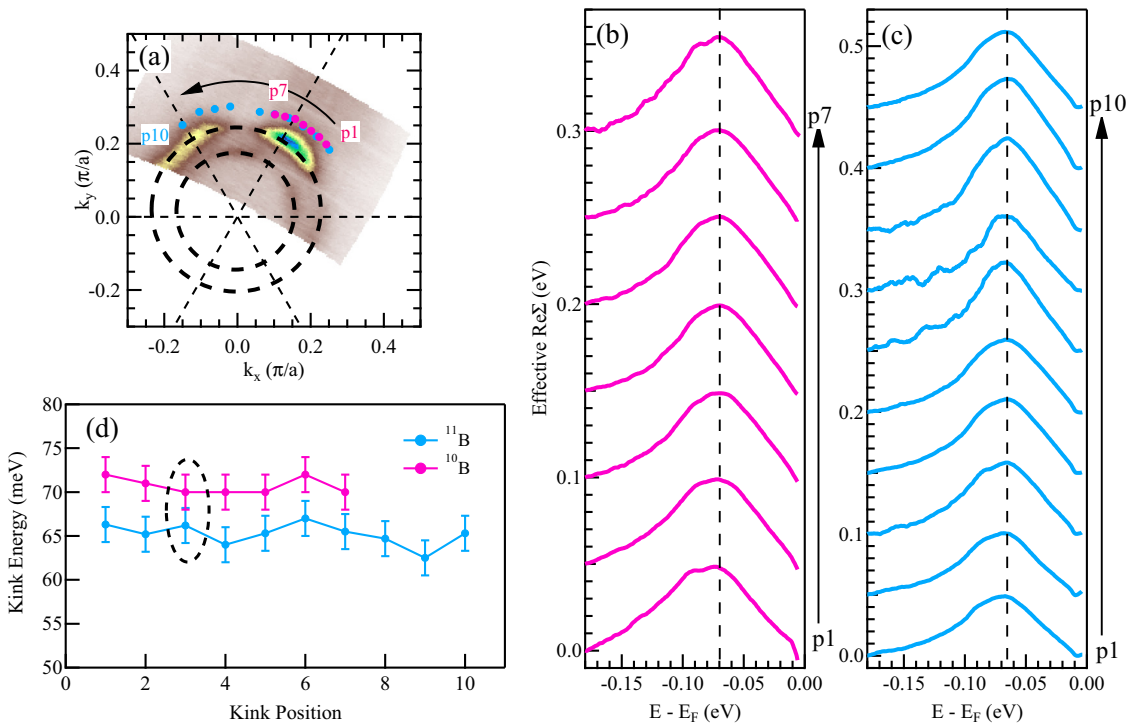

FIG. 2. Momentum dependence of the kink structure. (a) Measured Fermi surface of $Mg^{10}B_2$ at 40 K. [(b) and (c)] Momentum dependence of the effective ReΣ of outer σ band in $Mg^{10}B_2$ (b) and $Mg^{11}B_2$ (c). Data were taken at 20 K. (d) Momentum dependence of the kink energy obtained from (b) and (c). Corresponding kink structure positions in the Brillouin zone are mark with circles in (a). The data points in Fig. 1 are circled out.

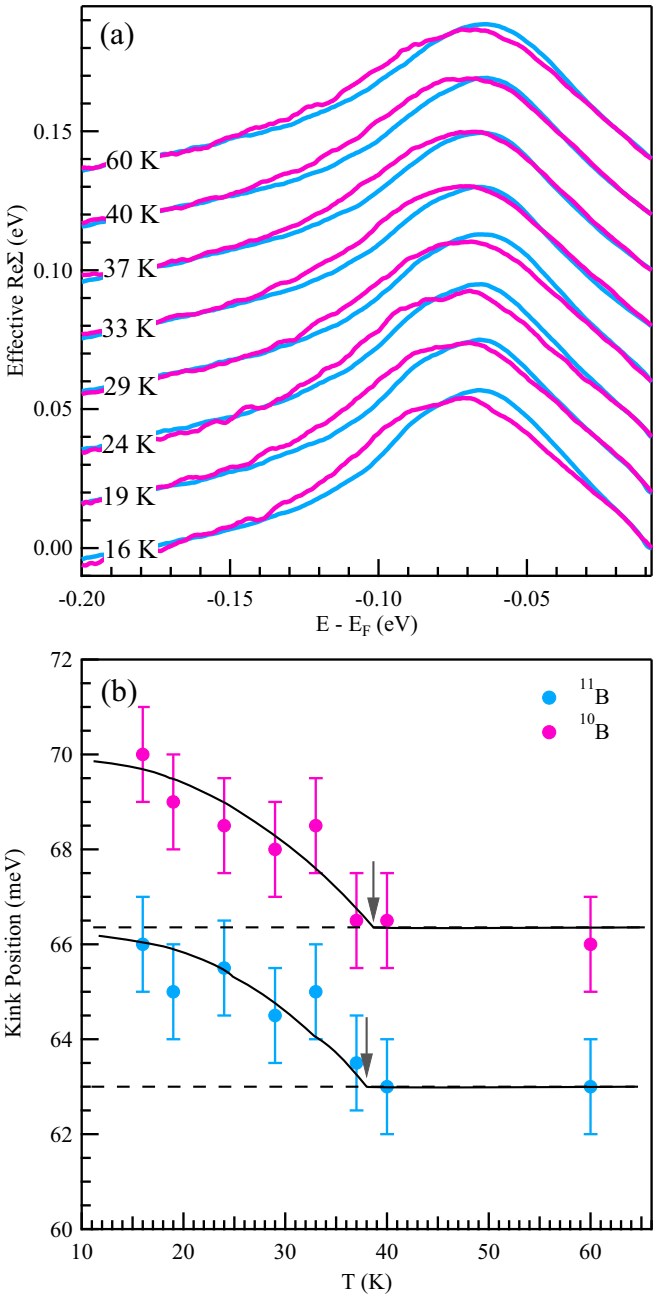

FIG. 3. Temperature dependence of the ReΣ for the samples made using two different boron isotopes. (a) Effective ReΣ for the outer σ band extracted from data measured at different temperatures. Cut position is the same as in Fig. 1. (b) Temperature dependence of the kink energy for the two isotopes. Solid lines are a guide for the eye. Arrows show corresponding transition temperatures from Fig. 1.

shifts towards a higher binding energy by ~3.5 meV, indicating that the isotope effect on kink structure is not affected by the superconducting transition in MgB_2. The lifetime of the quasiparticles in the σ band is expected to be dominated by intraband scattering [27]. If the kink position below T_c is at an energy of $\Omega_{2g} + \Delta_\sigma$ [28], the energy shift should be $\Delta_\sigma \sim 7$ meV. This number should be even larger once the hardening of the E_{2g} mode reported by Raman measurements is taken into consideration [29]. Further work is needed to understand why the kink energy shift below T_c is much reduced in MgB_2.

The partial isotope coefficient α_M is defined as $\alpha_M = -\frac{dlnT_c}{dlnM}$, where M is the atomic mass (see, for example, Ref. [6]). In standard BCS theory, α_M is equal to 1/2 [4], while the measured partial isotope coefficient of Boron in MgB_2 is substantially reduced to $0.26 \sim 0.31$ [6,7]. The deviation of α_B from standard 1/2 was previously interpreted as an effect of Coulomb repulsion pseudopotential (μ^*) or strong phonon-phonon interaction (phonon anharmonicity) [7,9,30]. Early theoretical [31] and experimental [32] results support the notion that large phonon anharmonicity exists in MgB_2 but were subsequently shown to be incorrect by theory and experiment [33,34] as well as in later reports [35,36]. In the harmonic limit, the phonon vibration frequency is directly proportional to the square root of the atomic mass. We can use the kink energies measured by ARPES, which represents the energy of the E_{2g} phonon in the two isotopic MgB_2 samples, to check the harmonicity of this mode. The ratio of the measured the kink energy ($\frac{\omega_{B11}}{\omega_{B10}} = \frac{63}{66} = 0.95 \pm 0.03$) is very similar to the inverse ratio of the square root of the B atomic mass for the two isotopes ($\sqrt{\frac{M_{B10}}{M_{B11}}} = \sqrt{\frac{10}{11}} = 0.95$). These results suggest that the E_{2g} phonon in MgB_2 is likely in the harmonic limit. Most likely, the above discrepancy is resolved when the two-phonon processes are taken into account [30].

In conclusion, we measured the isotope effect on the kink structure of the MgB_2 superconductor. A shift of 3.5 meV is revealed between kink structure energy for B^{10} and B^{11} samples. Although the kink position shows a slight change below T_c in both samples, the isotope effect on kink structure is not affected by a superconducting transition. Our results provide the first insights into the effects of the isotope substitution on electron-phonon interaction in a prototypical, conventional superconductor and will serve as baseline for understanding phonon effects in yet-to-be-discovered novel superconductors.

ACKNOWLEDGMENTS

We thank Igor Mazin for very useful comments. This work was supported by the U.S. Department of Energy, Office of Science, Basic Energy Sciences, Materials Science and Engineering Division. Ames Laboratory is operated for the U.S. Department of Energy by Iowa State University under Contract No. DE-AC02-07CH11358.

Raw data presented in this paper can be accessed at DOI: 10.17039/ameslab.dmse.2016DS5/1244493 (http://lib.dr.iastate.edu/ameslab_datasets/5).

[1] E. Maxwell, Phys. Rev. **78**, 477 (1950).
[2] C. A. Reynolds, B. Serin, W. H. Wright, and L. B. Nesbitt, Phys. Rev. **78**, 487 (1950).
[3] H. Fröhlich, Phys. Rev. **79**, 845 (1950).
[4] J. Bardeen, L. N. Cooper, and J. R. Schrieffer, Phys. Rev. **108**, 1175 (1957).
[5] J. Nagamatsu, N. Nakagawa, T. Muranaka, Y. Zenitani, and J. Akimitsu, Nature **410**, 63 (2001).

[6] S. L. Bud'ko, G. Lapertot, C. Petrovic, C. E. Cunningham, N. Anderson, and P. C. Canfield, Phys. Rev. Lett. **86**, 1877 (2001).
[7] D. G. Hinks, H. Claus, and J. D. Jorgensen, Nature **411**, 457 (2001).
[8] J. Kortus, I. I. Mazin, K. D. Belashchenko, V. P. Antropov, and L. L. Boyer, Phys. Rev. Lett. **86**, 4656 (2001).
[9] H. J. Choi, D. Roundy, H. Sun, M. L. Cohen, and S. G. Louie, Nature **418**, 758 (2002).
[10] J. P. Franck, in *Physical Properties of High Temperature Superconductors IV* (World Scientific, Singapore, 1994), p. 189.
[11] H. Keller, in *Superconductivity in Complex Systems*, edited by K. Müller and A. Bussmann-Holder (Springer, Berlin, 2005), Vol. 114, p. 143.
[12] R. H. Liu, T. Wu, G. Wu, H. Chen, X. F. Wang, Y. L. Xie, J. J. Ying, Y. J. Yan, Q. J. Li, B. C. Shi, W. S. Chu, Z. Y. Wu, and X. H. Chen, Nature **459**, 64 (2009).
[13] P. M. Shirage, K. Kihou, K. Miyazawa, C.-H. Lee, H. Kito, H. Eisaki, T. Yanagisawa, Y. Tanaka, and A. Iyo, Phys. Rev. Lett. **103**, 257003 (2009).
[14] A. Damascelli, Z. Hussain, and Z.-X. Shen, Rev. Mod. Phys. **75**, 473 (2003).
[15] G.-H. Gweon, T. Sasagawa, S. Zhou, J. Graf, H. Takagi, D.-H. Lee, and A. Lanzara, Nature **430**, 187 (2004).
[16] J. F. Douglas, H. Iwasawa, Z. Sun, A. V. Fedorov, M. Ishikado, T. Saitoh, H. Eisaki, H. Bando, T. Iwase, A. Ino, M. Arita, K. Shimada, H. Namatame, M. Taniguchi, T. Masui, S. Tajima, K. Fujita, S.-i. Uchida, Y. Aiura, and D. S. Dessau, Nature **446**, E5 (2007).
[17] H. Iwasawa, Y. Aiura, T. Saitoh, H. Eisaki, H. Bando, A. Ino, M. Arita, K. Shimada, H. Namatame, M. Taniguchi, T. Masui, S. Tajima, M. Ishikado, K. Fujita, S. Uchida, J. Douglas, Z. Sun, and D. Dessau, Physica C **463-465**, 52 (2007).
[18] H. Iwasawa, J. F. Douglas, K. Sato, T. Masui, Y. Yoshida, Z. Sun, H. Eisaki, H. Bando, A. Ino, M. Arita, K. Shimada, H. Namatame, M. Taniguchi, S. Tajima, S. Uchida, T. Saitoh, D. S. Dessau, and Y. Aiura, Phys. Rev. Lett. **101**, 157005 (2008).
[19] H. Uchiyama, K. M. Shen, S. Lee, A. Damascelli, D. H. Lu, D. L. Feng, Z.-X. Shen, and S. Tajima, Phys. Rev. Lett. **88**, 157002 (2002).
[20] S. Souma, Y. Machida, T. Sato, T. Takahashi, H. Matsui, S.-C. Wang, H. Ding, A. Kaminski, J. C. Campuzano, S. Sasaki, and K. Kadowaki, Nature **423**, 65 (2003).
[21] S. Tsuda, T. Yokoya, Y. Takano, H. Kito, A. Matsushita, F. Yin, J. Itoh, H. Harima, and S. Shin, Phys. Rev. Lett. **91**, 127001 (2003).
[22] D. Mou, R. Jiang, V. Taufour, R. Flint, S. L. Bud'ko, P. C. Canfield, J. S. Wen, Z. J. Xu, G. Gu, and A. Kaminski, Phys. Rev. B **91**, 140502 (2015).
[23] D. Mou, R. Jiang, V. Taufour, S. L. Bud'ko, P. C. Canfield, and A. Kaminski, Phys. Rev. B **91**, 214519 (2015).
[24] J. Karpinski, N. Zhigadlo, S. Katrych, R. Puzniak, K. Rogacki, and R. Gonnelli, Physica C **456**, 3 (2007).
[25] R. Cubitt, M. R. Eskildsen, C. D. Dewhurst, J. Jun, S. M. Kazakov, and J. Karpinski, Phys. Rev. Lett. **91**, 047002 (2003).
[26] R. Jiang, D. Mou, Y. Wu, L. Huang, C. D. McMillen, J. Kolis, H. G. Giesber, J. J. Egan, and A. Kaminski, Rev. Sci. Instrum. **85**, 033902 (2014).
[27] I. I. Mazin, O. K. Andersen, O. Jepsen, O. V. Dolgov, J. Kortus, A. A. Golubov, A. B. Kuz'menko, and D. van der Marel, Phys. Rev. Lett. **89**, 107002 (2002).
[28] A. W. Sandvik, D. J. Scalapino, and N. E. Bickers, Phys. Rev. B **69**, 094523 (2004).
[29] A. Mialitsin, B. S. Dennis, N. D. Zhigadlo, J. Karpinski, and G. Blumberg, Phys. Rev. B **75**, 020509 (2007).
[30] A. Y. Liu, I. I. Mazin, and J. Kortus, Phys. Rev. Lett **87**, 087005 (2001).
[31] T. Yildirim, O. Gülseren, J. W. Lynn, C. M. Brown, T. J. Udovic, Q. Huang, N. Rogado, K. A. Regan, M. A. Hayward, J. S. Slusky, T. He, M. K. Haas, P. Khalifah, K. Inumaru, and R. J. Cava, Phys. Rev. Lett. **87**, 037001 (2001).
[32] A. F. Goncharov, V. V. Struzhkin, E. Gregoryanz, J. Hu, R. J. Hemley, H.-k. Mao, G. Lapertot, S. L. Bud'ko, and P. C. Canfield, Phys. Rev. B **64**, 100509 (2001).
[33] M. Lazzeri, M. Calandra, and F. Mauri, Phys. Rev. B **68**, 220509 (2003).
[34] A. Shukla, M. Calandra, M. d'Astuto, M. Lazzeri, F. Mauri, C. Bellin, M. Krisch, J. Karpinski, S. M. Kazakov, J. Jun, D. Daghero, and K. Parlinski, Phys. Rev. Lett. **90**, 095506 (2003).
[35] M. Calandra, M. Lazzeri, and F. Mauri, Physica C **456**, 38 (2007).
[36] L. Simonelli, V. Palmisano, M. Fratini, M. Filippi, P. Parisiades, D. Lampakis, E. Liarokapis, and A. Bianconi, Phys. Rev. B **80**, 014520 (2009).